CHEMICAL ENGINEERING TRANSACTIONS
VOL. 109, 2024
A publication of AIDIC
The Italian Association of Chemical Engineering
Online at www.cetjournal.it
Guest Editors: Leonardo Tognotti, Rubens Maciel Filho, Viatcheslav Kafarov

ISBN 979-12-81206-09-0; **ISSN** 2283-9216
DOI: 10.3303/CET24109112

Morphology and Nanostructure of Soot Particles Emitted by a Domestic Boiler using Pine Pellets

Rosario Ballesteros[a], Sofía González-Correa[a], Esperanza Monedero[b], Rocío Collado[b], Magín Lapuerta[a]

[a]Escuela Técnica Superior de Ingeniería Industrial, Universidad de Castilla-La Mancha, Edificio Politécnica, Avda. Camilo José Cela, s/n. 13071. Ciudad Real. Spain.
[b]Instituto de Investigación en Energías Renovables, Universidad de Castilla-La Mancha, 02006 Albacete, Spain.
Magin.lapuerta@uclm.es

Particulate aerosols derived from combustion processes are a major contributor to climate change, but quantifying this effect is difficult because the optical and radiative properties of these aerosol depend on their composition, size, and structure. In the case of biomass boiler exhaust, five types of particles can be found in the chimney: soot agglomerates, organic films, organic particles with impregnated fibrous structures, condensed tars and condensed organic particles. All attention has so far been focused on the morphological and nanostructure characterization of soot agglomerates in internal combustion engines and in pre-mixed or diffusive flames. Similar works in boilers are scarce. In this work, the morphology and nanostructure of these agglomerates sampled in a domestic boiler using pine pellets is analysed. The relationship between the fractal dimension, the number of primary particles forming the agglomerate, the interlaminar distance and the degree of graphitization of these agglomerates versus diameter of gyration or electrical mobility diameter are presented.

1. Introduction

The role of biomass to produce thermal energy in the domestic sector has grown up progressively since it allows to ensure the energy supply through the use of household fuels, in addition to the obvious reduction of fossil fuel use. The EU Renewable Energy Directive (Directive (EU) 2023/2413) establishes that at least 42.5% of the final energy consumption should come from renewable sources. In the residential sector, biomass combustion in heating installations in the European Union represents about 17.3% in 2021 according to EUROSTAT, with pine pellets being the main feedstock due to its suitable properties (high heating value and low ash content) Biomass combustion processes in domestic boilers are not exempt from polluting emissions (Nussbaumer, 2010). Nussbaumer (2017) highlighted the importance of VOCs and the inhalable fraction of soot below 10 µm as the main relevant factors in air quality, although emissions of nitric oxide (NOx), polycyclic aromatic hydrocarbons (PAH), polychlorinated dibenzo-p-oxins and furans (PCDD/F) are also mentioned. According to several authors, the size, shape, morphology and chemical composition of soot particles are the most relevant aspects to be taken into account when assessing the potential impact of soot on the environment and humans. The environmental impact is inverse to particle size. The smaller they are, the more light they absorb and the less they scatter, and therefore they have higher heating potential. In addition, as the irregularity of the agglomerates grows, their surface area increases and, thus their capacity to adsorb hydrocarbons. For equal size, more irregular agglomerates (with lower fractal dimension) show higher absorption capacity. Moreover, as a carbonaceous material, soot varies greatly in their properties depending on the amount of sp^2 or sp^3 bonds it contains. There are many published studies that focus on the determination of the nanostructure and morphology of soot emitted by internal combustion engines (Lapuerta et al., 2023) (Arora et al., 2023) (Almanzalawy et al., 2023) or by premixed and diffusive flames (Chang et al., 2022) (Trivanovic et al., 2023). In more recent works, the optical characterization of such emissions has also been added, as it has an impact on radiative forcing. However, nanostructural and morphological analysis of soot emitted from boilers is scarce (Patiño et al., 2019) and there is a substantial lack.

Paper Received: 10 January 2024; Revised: 10 March 2024; Accepted: 2 April 2024
Please cite this article as: Ballesteros R., González-Correa S., Monedero E., Collado R., Lapuerta M., 2024, Morphology and Nanostructure of Soot Particles Emitted by a Domestic Boiler Using Pine Pellets, Chemical Engineering Transactions, 109, 667-672 DOI:10.3303/CET24109112

2. Experimental set-up

The experimental tests were performed on a fully monitored three-pass water-tube fixed-bed boiler with two thermal outputs of 25 kW and 55 kW. This is a domestic heating boiler with air staging and automatic ash removal. The complete system has been described extensively in previous work (Monedero et al., 2010) (Serrano et al., 2013). The feeding system consists of a hopper (previously calibrated for each biomass) where the biomass is loaded, and two synchronized feeding augers, which allows varying the biomass flow rate and thus the thermal load of the boiler. The excess air (λ) is defined as the actual air flow rate with respect to the stoichiometric one. The total air is divided into two flows: primary air (upward through the grate) and secondary air (through the wall orifices located just above the biomass bed). Two damper actuators operate the corresponding valves to adjust the desired primary air (PA)/secondary air (SA) ratio. The vibration frequency of the grate can be manually adjusted between 0 and 45 s to obtain adequate ash removal while avoiding disturbances in the bed resulting in fuel particles in the form of fly ash. These parameters were optimized for pine pellets in (Monedero et al., 2018) to achieve the highest boiler performance. The sampling probe for collecting particles is heated during all tests to prevent condensations along the sampling line and was connected at the chimney outlet. Prior to the soot collection, the exhaust is diluted with a dilution system composed of two dilutors from Dekati. Thermal insulation along the first dilution avoids hydrocarbon and water condensation on the aerosol surface. Each dilutor has a dilution ratio of 8:1, which considering the serial arrangement, gives a total dilution ratio of 64:1. The diluted flow is directed to the Differential Mobility Analyzer (DMA, model 3080, from TSI) to classify the aerosol particles. The selected mobility diameters were 10, 50, 215, and 350 nm. Samples of particle agglomerates were collected for each selected size with the electrostatic sampler ESPnano, from Dash Connector Technology on TEM grids (with 3 mm copper grids). TEM and HRTEM in lattice fringe mode was performed on the soot samples using a JEOL JEM-2100 electron microscope operating at 200 kV equipped with a LaB_6 filament. Figure 1 summarizes the protocol followed in this work, combining on-line and off-line measurements. The microscopic images obtained from the grids with the electrostatic sampler were pre-processed to obtain the diameter of gyration (d_g), the projected area of the agglomerates (A_p), and the average diameter of primary particles (d_{p0}). With this information, the fractal dimension (D_f), the prefactor (k_f) and the number of primary particles (n_{p0}) were calculated using homemade software (Lapuerta et al., 2006). The high-resolution microscopy images were subjected to a skeletonization process (using ImageJ, free software) to calculate the interlaminar distance (d_{002}) and the degree of graphitization of the samples (g), following the proposal by Atria el al. (2002). All morphology-related results of the agglomerates are compared with previous results (with hollow circles) obtained in a parallel study carried out on a vehicle placed on a rolling test bench (Lapuerta et al., 2023).

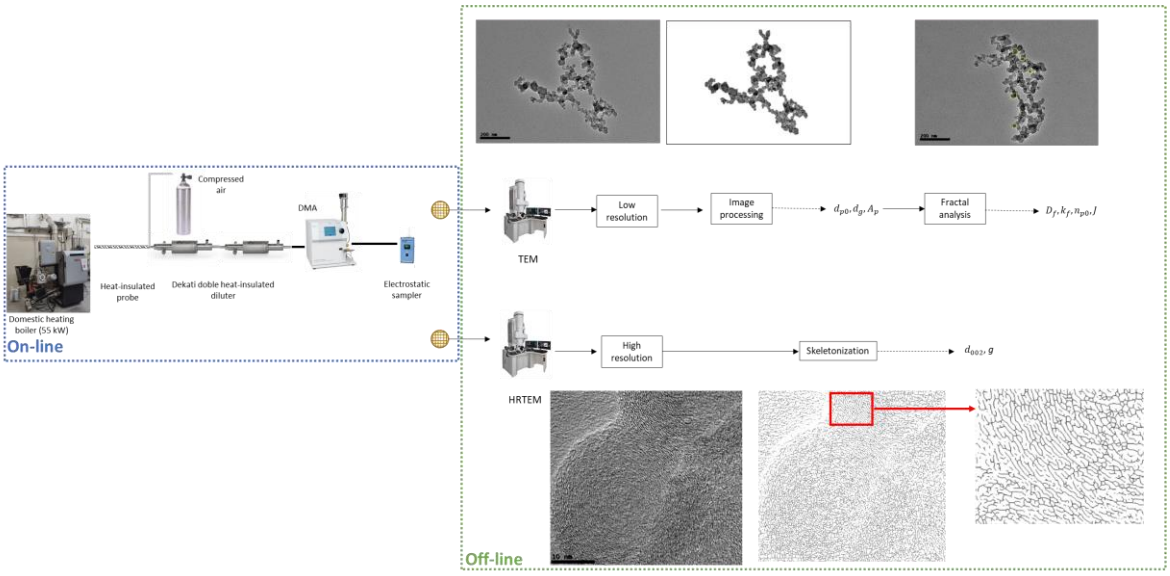

Figure 1. Experimental outline, including on-line measurements, off-line measurements, and processing.

3. Results and discussion

3.1. Relationship between soot equivalent diameters

The relationship between the electrical mobility diameter (d_{em}) of the soot agglomerates selected with the DMA and the diameter of gyration (d_g) obtained from the collection and subsequent analysis of microscopy images is shown in Figure 2. This figure shows the relationship between agglomerate diameters in the boiler (squares) and those obtained in a vehicle (hollow circles). In both cases, the standard deviation is larger with increasing agglomerate size. This variability could be reduced by increasing the number of clusters collected. It can be also observed that the regression line deviates from the bisector (which represents perfect correspondence between both diameters) for both low and high mobility diameters, leading to an underestimation of d_{em} for low sizes and to an overestimation of d_{em} for large agglomerates. Two reasons may explain this discrepancy: 1. The composition of small agglomerates have more variable composition than that of larger agglomerates. The electrical mobility of the agglomerates depends on the composition and even more so if these agglomerates contain metals (as in the case of fly ash in boiler chimneys outlet). 2. The inhomogeneity in soot morphology can cause particles of similar size to experience different amounts of drag in the DMA, which changes their electrical mobility, which is shape dependent. None of these factors can be considered systematic (the composition of the agglomerates cannot be controlled), so they all contribute to the previously mentioned variability. The similarity between d_g and d_{em} is higher for the agglomerates from the vehicle than for those emitted by the domestic boiler, probably also due to the two reasons mentioned above, which can be summarized in a higher compositional diversity of the agglomerates for the boiler.

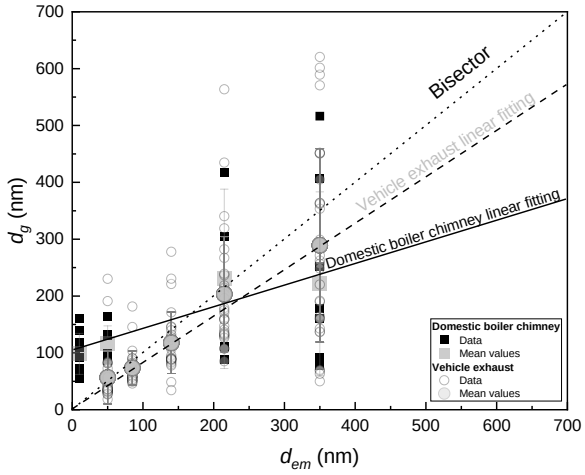

Figure 2. Relationship between diameter of gyration and mobility diameter (data, mean values and fittings).

3.2. Morphology

Figure 3a shows the relationship between A_p and d_g (compared with vehicle agglomerates in hollow circles). The diameter of gyration scales to the projected area with a power of 1.49 for boiler agglomerates. This exponent describes the average internal arrangement of the primary particles in the agglomerate image. It can be associated with the planar fractal dimension (i.e., the fractal dimension of the projected image), which ranges from 1 to 2. This exponent is lower than that observed for vehicle agglomerates, 1.65. Figure 3b shows that, in general, the primary particles are larger for larger agglomerates. The exponent obtained in the correlation between the diameter of the primary particles and the diameter of gyration of the agglomerates (0.3) is similar than that observed for agglomerates emitted by vehicles (also 0.3) and slightly higher than that proposed by Olfert and Rogak (Olfert and Rogak, 2019) for agglomerates emitted by flames (0.35). As shown in Figure 4a, D_f decreases with increasing diameter of gyration. This trend is represented by a potential regression. The dispersion of D_f values decreases with increasing size for both boiler and vehicle agglomerates. Fractal dimensions less than 2 (in the interval 1-3) are obtained for agglomerates with diameters of gyration larger than 100 nm, implying that their structure is quite far from a compact object, revealing that conceiving soot agglomerates as spherical particles can lead to misconceptions. The fractal dimension and the prefactor represent different roles in the description of an agglomerate. While the fractal dimension quantifies the irregularity/clustering of the agglomerate structure (with an exponent), the prefactor expresses how the primary particles are clustered independent of their size (with a linear factor). As shown in Figure 4b, the prefactor increases rapidly (faster for boiler agglomerates than for vehicle *ones*) with d_g up to a value of about 200 nm, after which it remains almost constant at about 1.8, for both agglomerate types. Aiming to quantify the

contribution of the number of primary particles (n_{p0}) to the differences between mobility and gyration diameters, Figure 5 shows the behavior of the d_{em}/d_g ratio against n_{p0}. The proposal by Kelesidis & Kholghy (2021), that statistically relates d_{em} and d_g as a function of n_{p0} for flames, and that by Lapuerta et al. (2023) for vehicle agglomerates, fall away from the trend observed for boiler agglomerates.

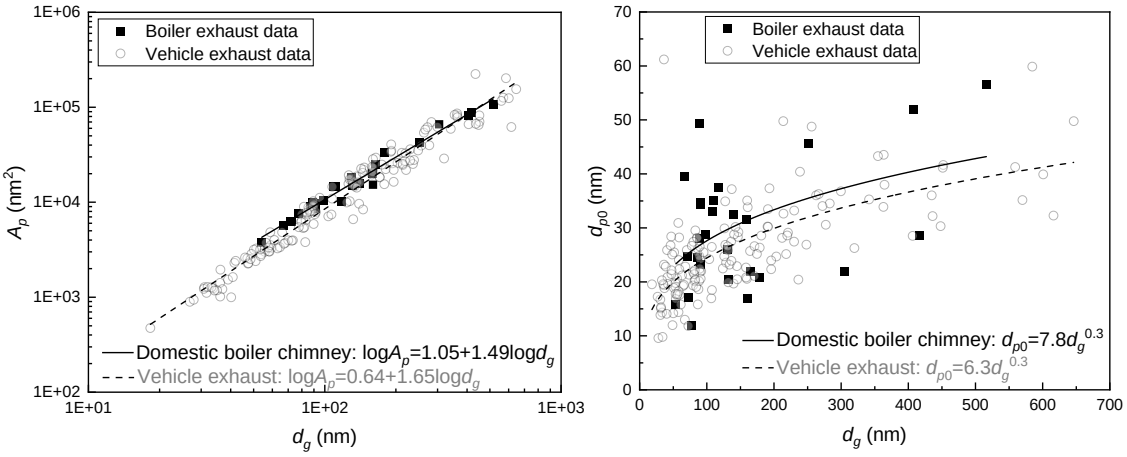

(a) *(b)*

Figure 3. (a) Logarithmic relationship between projected area and diameter of gyration (b) Relationship between diameter of primary particles and diameter of gyration of agglomerates.

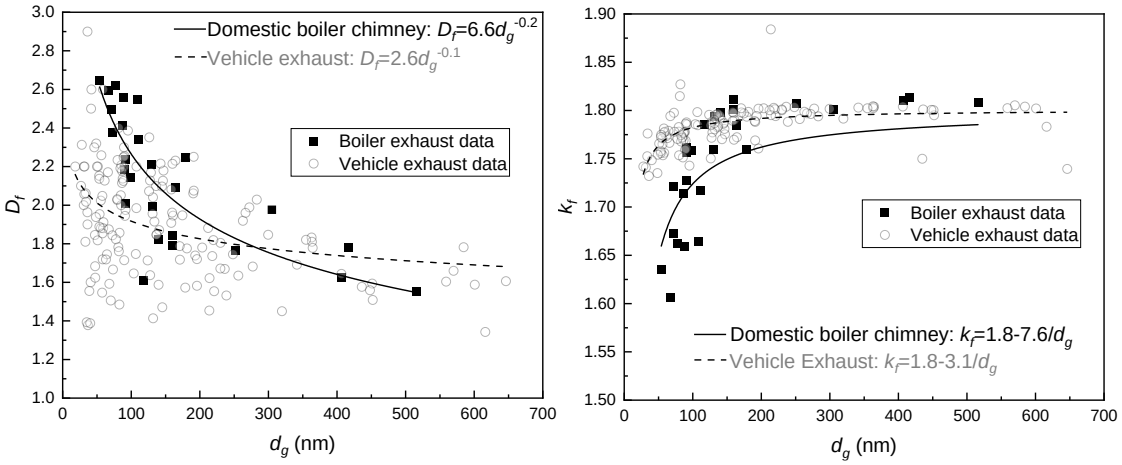

(a) *(b)*

Figure 4. (a) Relationship between fractal dimension and diameter of gyration of agglomerates, (b) Relationship between prefactor and diameter of gyration of agglomerates.

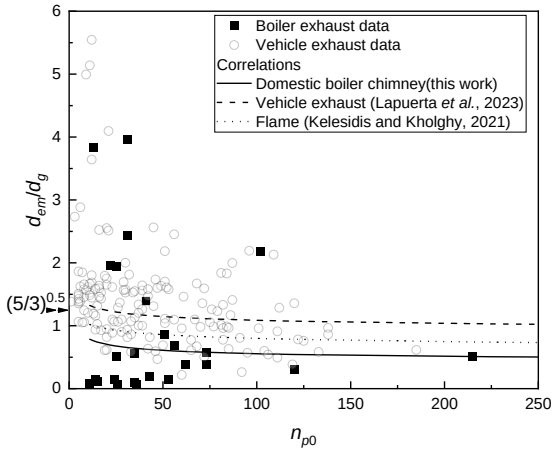

Figure 5. Relationship between the ratio d_{em}/d_g and the number of primary particles, and comparison with those proposed by Kelesidis & Kholghy, 2021 and by Lapuerta et al., 2023.

3.3. Nanostructure

From high-resolution TEM images (HRTEM), the pattern of graphitic-like layers in the nanostructure of the soot agglomerates soot can be visualized. Among other parameters, the nanoscale organization of soot can be described with the interlaminar distance (d_{002}), from which a degree of graphitization (g) in these arrangements can be quantified. Although HRTEM images are 2D projections of 3D volumes, due to the concentric symmetry of most soot nanoparticles, the geometrical properties measured in 2D images can be easily extrapolated to 3D. From the high-resolution skeletonized micrographs, it is possible to obtain the interlaminar distance and thus the degree of graphitization of the samples (Figures 6a and 6b). The interlaminar distance presents a maximum of approximately 3.74 for d_{em}=214 nm (and therefore, a minimum degree of graphitization). Consequently, the degree of graphitization shows a minimum value in this range (medium-size agglomerates).

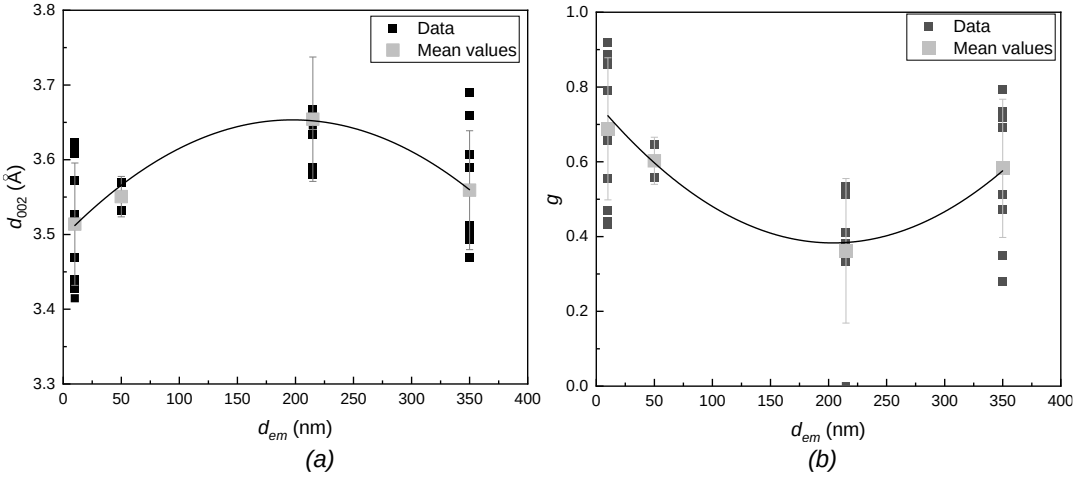

Figure 6. Relationship between interlaminar distance (a) degree of graphitization (b) and electrical mobility diameter of agglomerates.

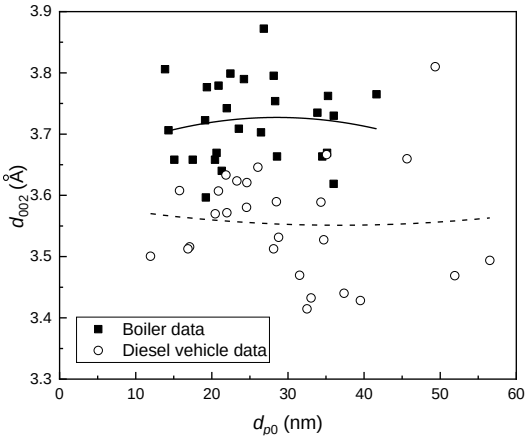

Figure 7. Relationship between interlaminar distance and average diameter of primary particles.

Trying to explain this behavior, the interlaminar distances are represented in front of the diameter of the primary particles in Figure 7. It can be observed that these distances are, in general, larger than those observed in soot agglomerates sampled from the vehicle exhaust tube, consistently with the lower temperatures reached in the boiler than in the combustion chamber of the vehicle engine. However, no clear trend has been found (neither for soot sampled from the vehicle nor from the boiler) with the primary particle diameter. Therefore, the expected higher amount of amorphous carbon consistent with the higher torsional strength imposed by the higher curvature of the graphitic layers in small particles (Vander Wal and Tomasek, 2003) could not be confirmed.

4. Conclusions

The morphology of the agglomerates collected in the chimney of a biomass boiler shows a different morphological pattern than the agglomerates collected from the exhaust of an internal combustion vehicle. The differences between the diameter of gyration and the electrical mobility diameter of the agglomerates are much

larger than in the case of vehicle exhaust. These discrepancies are due to the higher variability in the composition of these clusters leading to a completely different electrical mobility than that of agglomerates composed exclusively of soot. The degree of graphitization of agglomerates in the boiler outlet is lower than in the vehicle exhaust. Despite the relatively limited number of agglomerate data obtained from the boiler, it can be reasonably anticipated that it will be difficult to find universal fits for soot agglomerates from different sources (e.g., diesel engines, gas turbines, or heating boilers), since both the combustion conditions and the fuels used are very different. To confirm this, larger datasets need to be obtained.

Nomenclature

A_p - projected area, nm^2
d_{002} - interlaminar distance, Å
d_{em} - electrical mobility diameter, nm
d_g - diameter of gyration, nm
d_{p0} - primary particle diameter, nm
D_f - fractal dimension
n_{p0} -number of primary particles
g - degree of graphitization
k_f - prefactor
λ - excess air
PA - primary air
SA - secondary air
TEM - Transmission Electric Microscopy
HRTEM - High Resolution TEM

Acknowledgements

The Ministry of Science and Innovation from Spain is gratefully acknowledged for funding project RAD-SOOT (ref. PID 2019–109767RB-I00).

References

Almanzalawy, M.S., Elkady, M.F., Mori, S., Elwardany, A.E. Quantification of soot nanostructure produced from a diesel engine fueled with C3 ketone. Energy, 2781, (Article number 127790), 2023. https://doi.org/10.1016/j.energy.2023.127790.

Arora, P.A., Verma, P., Zare, A., Lodi, F., Jafari, M., Stevanovic, S., Bodisco, T.A., Brown, R.J., Ristovski, Z. Morphology and nanostructure of soot particles from diesel engine under transient and steady-state operating conditions with a microalgae fuel component, dioctyl phthalate biofuel. Sustainable Energy Technologies and Assessments, 60, (Article number 103504), 2023. https://doi.org/10.1016/j.seta.2023.103504.

Atria, J.V., Rusinko Jr, F., Schobert, H.H. Structural ordering of Pennsylvania anthracites on heat treatment to 2000-2900 ºC. Energy and Fuels 16 (6), 1343–1347, 2002. https://doi.org/10.1021/ef010295h.

Chang, D., Li, J., Yang, Y., Gan, Z. Soot Morphology and Nanostructure Differences between Chinese Aviation Kerosene and Algae-Based Aviation Biofuel in Free Jet Laminar Diffusion Flames. ACS Omega, 12, 7 (14), 11560–11569, 2022. https://doi.org/10.1021/acsomega.1c05125.

Collado, R., Monedero, E., Casero-Alonso, V.M., Rodríguez-Aragón, L.J., Hernández, J.J. Almond shells and exhausted olive cake as fuels for biomass domestic boilers: optimization, performance and pollutant emissions. Sustainability, 14, 7271, 2022. https://doi.org/10.3390/su1412727.

Directive (EU) 2018/2001 on the Promotion of the Use of Energy from Renewable Sources; 2018; pp. 141–144. Consolidated.https://eur-lex.europa.eu/legalcontent/EN/TXT/?uri=CELEX%3A02018L2001 20220607 (accessed on 28 November 2023).

EUROSTAT, 2021. Final energy consumption by sector. https://ec.europa.eu/eurostat/web/main/data/database (accessed on 11 December 2023)

Lapuerta, M., Ballesteros, R., González-Correa, S. Relationships between morphology and optical properties of vehicle-emitted soot. Journal of Aerosol Science, 174, (Article number 106261), 2023. https://doi.org/10.1016/j.jaerosci.2023.106261.

Lapuerta, M., Ballesteros, R., Martos, F.J. A method to determine the fractal dimension of diesel soot agglomerates. Journal of Colloid Interface Science, 303 (1), 149-158, 2006. https://doi.org/10.1016/j.jcis.2006.07.066.

Monedero, E., Portero, H., Lapuerta, M. Combustion of poplar and pine pellet blends in a 50 kW domestic boiler: Emissions and combustion efficiency. Energies, 11, 1580, 2018. https://doi.org/10.3390/en11061580.

Nussbaumer, T. Overview on technologies for biomass combustion and emission levels of particulate matter, 2010. Swiss Federal Office for the Environment (FOEN), Zürich, Switzerland.

Nussbaumer, T. Aerosols from biomass combustion. Technical report on behalf of the IEA Bioenergy Task 32. (pp. 32), 2017. Verenum Research, Zurich, and Lucerne University of Applied Sciences and Arts, Horw, Switzerland.

Olfert, J., Rogak, S. Universal relations between soot effective density and primary particle size for common combustion sources. Aerosol Science and Technology, 485-492, 53, 5, 2019. https://doi.org/10.1080/02786826.2019.1577949.

Patiño, D., Pérez-Orozco, R., Porteiro, J., Lapuerta, M. Characterization of biomass PM emissions using thermophoretic sampling: Composition and morphological description of the carbonaceous residues. Journal of Aerosol Science, 127, 49-62, 2019. https://doi.org/10.1016/j.jaerosci.2018.10.005.

Serrano, C., Portero, H., Monedero, E. Pine chips combustion in a 50 kW domestic biomass boiler. Fuel, 111, 564–573, 2013. https://doi.org/10.1016/j.fuel.2013.02.068.

Trivanovic, U., Pereira Martins, M., Benz, S., Kelesidis, G. A., Pratsinis, S. E. Dynamics of soot surface growth and agglomeration by enclosed spray combustion of jet fuel. Fuel, 34215, (Article number 127864), 2023. https://doi.org/10.1016/j.fuel.2023.127864.

Vander Wal, R. L., Tomasek, A. J. Soot oxidation: dependence upon initial nanostructure. Combustion and Flame, 134 (1–2), 1-9, 2003. https://doi.org/10.1016/S0010-2180(03)00084-1.